Catalytic lignocellulose biorefining in *n*-butanol/water: a one-pot approach toward phenolics, polyols, and cellulose†

T. Renders, [iD] *[a] E. Cooreman,[a] S. Van den Bosch, [iD] [a] W. Schutyser, [iD] [a] S.-F. Koelewijn, [iD] [a] T. Vangeel,[a] A. Deneyer,[a] G. Van den Bossche,[a] C. M. Courtin[b] and B. F. Sels [iD] *[a]

Lignocellulose constitutes an alluring renewable feedstock for the production of bio-based chemicals. In this contribution, we propose a chemocatalytic biorefinery concept that aims to convert lignocellulosic biomass (*Eucalyptus* sawdust) into (i) lignin-derived (mono)phenolics, (ii) hemicellulose-derived polyols, and (iii) a cellulose pulp. This is achieved by processing biomass in an equivolumetric mixture of *n*-butanol and water at elevated temperature (200 °C), in the presence of Ru/C and pressurised hydrogen (30 bar). During this one-pot *Reductive Catalytic Fractionation* (RCF) process, the hot liquor enables the extraction and solvolytic depolymerisation of both lignin and hemicellulose, while the catalyst and reductive environment are essential to hydrogenate reactive intermediates (coniferyl/sinapyl alcohol and sugars) toward stable target products (phenolics and polyols, respectively). After the catalytic reaction, the solid carbohydrate pulp (mainly cellulose) is easily retrieved upon filtration. Phase separation of *n*-butanol and water occurs upon cooling the liquor (<125 °C), which offers a facile and effective strategy to isolate lignin-derived phenolics (*n*-butanol phase) from polyols (aqueous phase). The three resulting product streams provide a versatile platform for down-stream conversion, *en route* to bio-based chemicals. A proof-of-concept experiment using a 2 L batch reactor demonstrates the scalability potential. Furthermore, this contribution highlights that the conversion of each biopolymer is influenced in a different way by reaction parameters like catalyst, hydrogen pressure, temperature, and acidity (HCl). The key challenge is to find suitable conditions that allow (close-to-)optimal valorisation of all constituents.

Introduction

Lignocellulosic biomass is regarded as a promising resource for the bio-economy.[1,2] Within this context, utilising lignocellulose as a renewable feedstock for the production of chemicals is an aspiring opportunity.[3–10] A *lignocellulose-to-chemicals* valorisation chain often starts with biomass fractionation, *i.e.* turning raw biomass into well-defined product streams that can serve as a versatile and sustainable platform for the chemical industry.

A wide variety of lignocellulose fractionation processes have been disclosed over the past 50 years,[3,11] with many of them being geared to obtain maximal revenue from the carbohydrate fraction. This exclusively carbohydrate-oriented focus is becoming out-dated as newly proposed fractionation techniques aim to obtain added-value from the entire biomass, including lignin. Lignin is a complex phenolic biopolymer and is particularly interesting for the production of aromatic chemicals.[3,10,12–14] Its monomer units have a characteristic substitution pattern, which can provide beneficial features to targeted end products, like for instance reduced estrogenic potency.[15,16] Despite being a promising resource, lignin is prone to undergo irreversible condensation during its isolation,[17] which is a root cause for ineffective depolymerisation. Hence, minimising condensation during the early stages of biorefining is essential to construct a successful *lignin-to-chemicals* value chain.[12,18]

Lignin can be isolated with minor structural alteration by applying specific media that enable mild process conditions, for instance liquid ammonia,[19–21] *γ*-valerolactone,[22,23] ionic liquids,[24–26] and certain organosolv systems.[27–32] An alternative concept is to prevent lignin condensation 'actively',[18] as recently exemplified by the stabilisation of lignin with alde-

[a]Center for Surface Chemistry and Catalysis, KU Leuven, Celestijnenlaan 200F, 3001 Leuven, Belgium. E-mail: tom.renders@kuleuven.be, bert.sels@kuleuven.be

[b]Center for Food and Microbial Technology, KU Leuven, Kasteelpark Arenberg 22, 3001 Leuven, Belgium

hydes during its extraction from beech and poplar wood.[33,34] Both strategies provide a solid lignin product that is much more reactive towards subsequent depolymerisation than traditional lignin (*e.g.* Kraft, soda), consequently resulting in higher monomer yields and selectivities.[19,22,28,33–36]

A different approach to (actively) circumvent the problem of lignin condensation, is to combine biomass fractionation with instantaneous lignin disassembly and stabilisation.[18] This strategy is applied in the *Reductive Catalytic Fractionation* (RCF) of lignocellulose,[37–41] or also termed *Catalytic Upstream Biorefining* (CUB).[12,42,43] During RCF, native lignin is solvolytically extracted from the biomass, followed by immediate depolymerisation and reductive stabilisation.[38,44–46] The latter step requires a redox catalyst (*e.g.* Ru/C, Pd/C, Ni/C),[45,47–50] and results in a highly depolymerised lignin oil containing phenolic monomers in close-to-theoretical yields,[44,51] in addition to dimers and short oligomers.[37,50] The cellulosic carbohydrates remain preserved in the solid fraction, and can easily be retrieved as a pulp upon filtration of the reaction mixture.[37,42,43,45,49]

The hemicellulose fraction can either be (i) retained in the pulp or (ii) solubilised together with the lignin fraction.[39–41,52–55] The first scenario requires precise tuning of the reaction conditions to find an optimal balance between lignin removal and hemicellulose preservation.[52,55] Alternatively, simultaneous extraction of hemicellulose and lignin can be pursued to yield a cellulosic pulp, and is enabled by performing RCF in mildly acidic and/or aqueous media.[39–41,52–55] Under these conditions, degradation of hemicellulose sugars can occur,[40,53] resulting in a less efficient utilisation of the biomass. A possible solution would be to exploit the reductive catalytic system to simultaneously convert solubilised hemicellulose into polyols *via* hydrolytic hydrogenation. Pentitols (C5) and hexitols (C6) are more stable than their parent sugars, and are widely conceived as a promising platform for bio-based chemicals.[56–58] Hydrolytic hydrogenation has already been studied using pure cellulose,[57,59–63] isolated hemicellulose,[64–69] and raw/pretreated biomass,[70–74] though it has not yet been pursued in the context of RCF. Integrated hydrolytic hydrogenation of hemicellulose is expected to require precise tuning of process conditions.[65] Moreover, simultaneous depolymerisation of lignin and hemicellulose into soluble products (*i.e.* phenolics and polyols) necessitates an efficient down-stream separation strategy.

We herein propose and investigate an innovative catalytic biorefinery concept, targeting the one-step fractionation of raw woody biomass into three valuable product streams: (i) lignin-derived phenolics, (ii) hemicellulose-derived polyols, and (iii) a cellulosic pulp (Fig. 1). In order to provide an integrated separation approach of the solubilised products, RCF is performed in an equivolumetric mixture of *n*-butanol and water. After the reaction, the limited miscibility of *n*-butanol and water can be exploited to separate lignin-derived phenolics (preferentially in *n*-butanol phase) from the more polar polyols (preferentially in aqueous phase). Noteworthy, the upper critical solution temperature (UCTS) of *n*-butanol/water equals *circa* 125 °C,[75] which implies that any *n*-butanol/water mixture is monophasic at typical RCF reaction temperatures (≥160 °C). Because of this dual behaviour, the intrinsic complexity of a biphasic solvent system is omitted, while still exploiting the benefits of an integrated product separation after reaction. In fact, a truly biphasic solvent system during (batch) RCF would require substantial efforts to provide adequate dispersion and mass transfer between the different phases, especially since a solid catalyst and a solid substrate (with high volumetric loading) are involved. Also when performing RCF in flow-through mode, as was recently disclosed,[38,46,76] a monophasic solvent system is expected to be more appropriate.
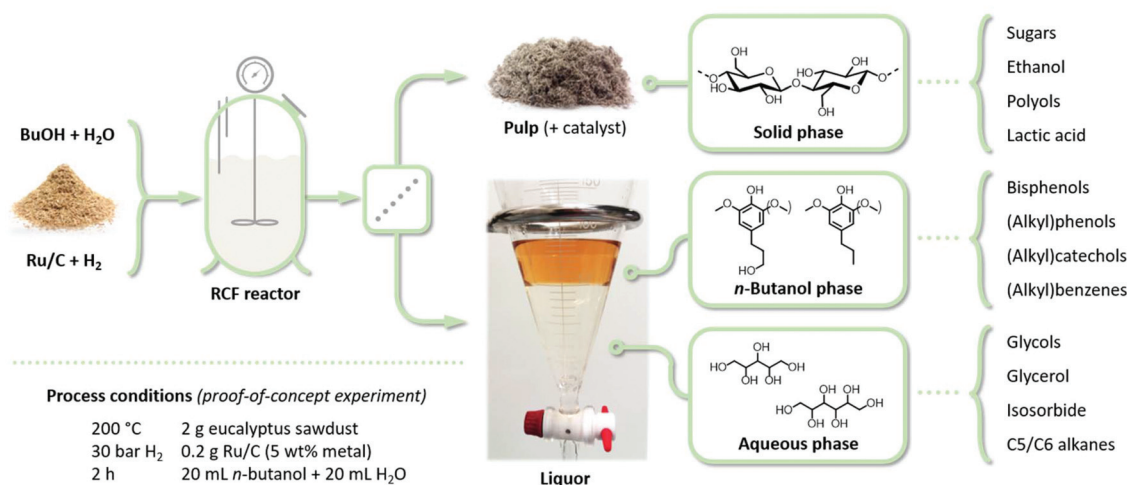

Fig. 1 General scheme of the *n*-butanol/water RCF process targeting (i) a cellulosic pulp, (ii) lignin-derived phenolics, and (iii) hemicellulose-derived polyols. The *n*-butanol/water mixture is monophasic during the reaction (200 °C), but biphasic below the UCST (125 °C). This dual behaviour offers an integrated separation approach of the solubilised products, while omitting the complexity of a biphasic solvent system during reaction. For each product stream, a few valorisation opportunities are presented.

Results and discussion

Proof-of-concept

A general scheme of the *n*-butanol/water RCF process is presented in Fig. 1. To demonstrate the concept, 20 mL *n*-butanol, 20 mL water, and 0.2 g of Ru/C catalyst powder were added to a 100 mL Parr batch reactor, together with 2 g of pre-extracted eucalyptus sawdust. The composition of the eucalyptus substrate is summarised in Table S1.† The mixture was pressurised with hydrogen (30 bar), stirred (750 rpm), and heated to a reaction temperature of 200 °C for 2 h. After cooling, the reactor contents were quantitatively collected and filtered. The residual solids (pulp and catalyst) were washed with additional water and *n*-butanol. The resulting pulp yielded 50.4 wt% of the initial biomass and retained most of the cellulose (96 wt% retention), whereas the major part of the hemicellulose was removed (85 wt% solubilisation). The filtrate instantly separated into an organic and aqueous phase (Fig. 1), containing depolymerised lignin and hemicellulose, respectively, thereby providing a facile and effective separation of the solubilised products (Fig. S1, see ESI† for experimental procedures). Evaporation of *n*-butanol yielded a viscous oil, which after drying measured 22.2 wt% of the initial biomass weight. The weight of the *n*-butanol oil is close to the total lignin content of the eucalyptus sawdust (22.9 wt%), indicating extensive lignin extraction from the biomass.

The obtained lignin oil (from the *n*-butanol phase) is rich in phenolic monomers, corresponding to a yield of 48.8 wt%, as measured by GC-FID and based on total lignin content of the pre-extracted eucalyptus sawdust. The monomer products mainly comprise propanol-substituted syringol (S) and guaiacol (G), with a smaller fraction consisting of propyl- and ethyl-substituted analogues (Fig. 2A). Noticeably, previous work on Ru/C-catalysed RCF reported the selective formation of propyl-G/S when processing sawdust in pure methanol at 250 °C.[48] This discrepancy demonstrates that process conditions (temperature, solvent) can exert a strong effect on product selectivity (see also Fig. S2 and 3† for verification).

The molecular weight distribution of the lignin-derived products in the *n*-butanol phase was assessed by gel permeation chromatography (GPC). The GPC chromatogram depicted in Fig. 2C shows that the organic phase contains monomers, dimers, trimers, and small oligomers. The largest oligomers elute at 7 min, which corresponds to a M_w of 1850 g mol^{-1} (DP of *circa* 10). Additionally, GPC corroborates the prevalence of propanol-substituted monomers, in alignment with GC-FID analysis. HSQC NMR (Fig. 2D) and ^{13}C NMR (Fig. S7†) support the identification of the obtained products, and furthermore evidence the almost complete absence of residual inter-unit ether bonds. Hence, we conclude that lignin undergoes effective and selective depolymerisation in the proposed *n*-butanol/water RCF system.

The products in the aqueous phase were analysed by GC-FID following trimethylsilylation to increase volatility (ESI†). Products detected by GC-FID mainly include C5 polyols (48 mg g$_{biomass}^{-1}$), C6 polyols (10 mg g$_{biomass}^{-1}$), and smaller
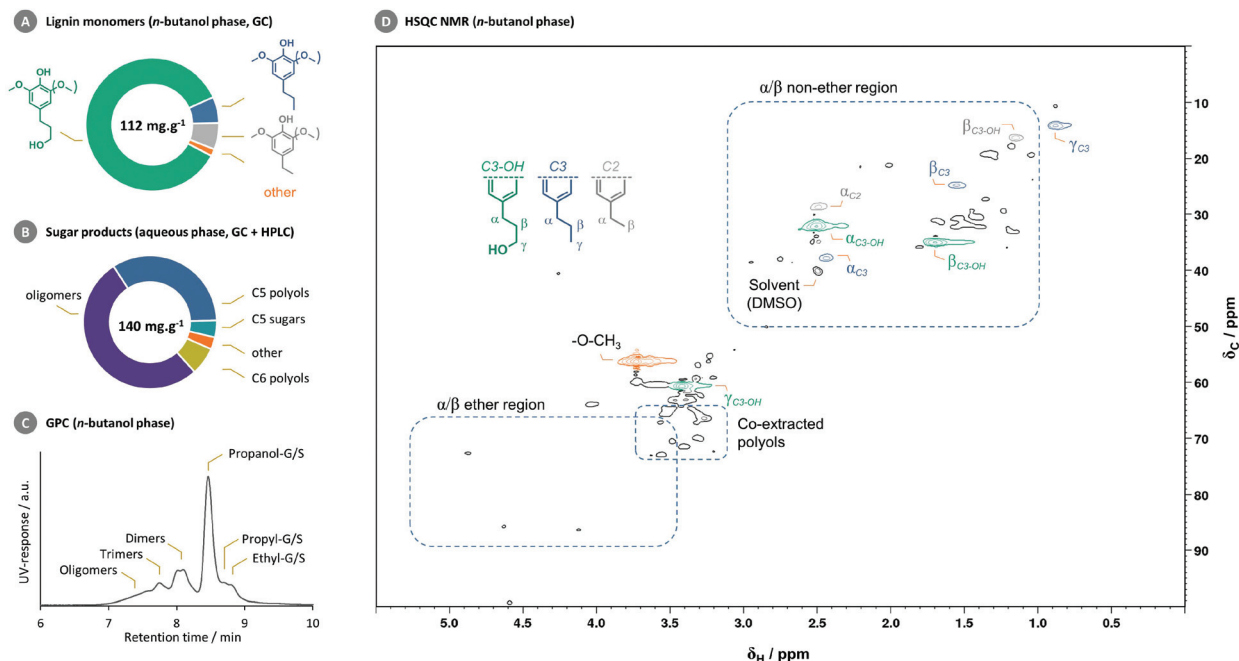

Fig. 2 Analysis of the *n*-butanol phase and aqueous phase obtained from Ru/C-catalysed RCF of eucalyptus. Reaction scheme and conditions: See Fig. 1. (A) Lignin monomer yield, expressed as mg$_{monomers}$ per g$_{biomass}$. (B) Yield of sugar products in aqueous phase, expressed as mg per g$_{biomass}$. See Fig. S20† for HPLC analysis. (C) GPC analysis. Signal assignment is based on analytical standards and self-synthesised dimers and trimers (Fig. S11†). (D) HSQC NMR. The presence of trace amounts of polyols is due to repeated extraction of the aqueous phase with *n*-butanol (3 cycles), but can be minimised by optimisation of the extraction procedure (Fig. S1†).

quantities of non-reduced C5/C6 sugars, glycerol, propane diol, and ethylene glycol (Fig. 2B). The C5 polyol fraction mainly comprises xylitol (89%), in addition to arabitol (11%). HPLC was performed to identify non-volatile products present in the aqueous phase. Signals corresponding to oligomers were observed (Fig. S20†), equalling 73 mg $g_{biomass}^{-1}$. The combined yield of C5 polyols, C5 sugars, and oligomers is equivalent to 74% of the initial biomass C5 content (mainly xylan, Table S1†). A general overview of the fate of the main lignocellulose constituents is presented in Fig. 3.

To demonstrate the scalability potential of the process, an experiment was performed using a 2 L Parr batch reactor (*i.e.* a 20-fold increase of the reactor volume, Fig. S4A†). The reactor was loaded with 80 g non-extracted eucalyptus sawdust (×40), 8 g Ru/C (×40), 400 mL *n*-butanol and 400 mL water (×20). Note that the biomass-to-solvent ratio is two times higher compared to the small scale reference experiment, which is more desirable for industrial operation. The results of the 2 L scale experiment in relation to the 100 mL reference are summarised in Fig. S5 of the ESI.† The obtained pulp equals 50.9 wt% of the initial biomass, being quasi-similar to the pulp yield on the small scale (50.4 wt%). A high lignin monomer yield was achieved (43.7 wt%) with a 79 wt% selectivity towards propanol-substituted compounds, which was confirmed by GPC analysis (Fig. S5A and B†). The yield of C5 polyols (67 mg $g_{biomass}^{-1}$) on the other hand is higher than the small scale reference experiment (48 mg $g_{biomass}^{-1}$). This discrepancy is ascribed to the higher biomass-to-solvent ratio, which was verified on 100 mL scale (Fig. S5C†). We reason that a higher biomass-to-solvent ratio leads to a slightly lower pH due to deacetylation of hemicellulose, in line with a study by Rinaldi and co-workers.[43] Mildly acidic media facilitate the conversion of hemicellulose to C5 and C6 polyols (*vide infra*).

Influence of the redox catalyst

To illustrate the importance of the Ru/C catalyst, the *n*-butanol/water RCF process was performed with other noble metal catalyst. Pd/C, Pt/C, and Rh/C catalyst powders (5 wt% metal loading) were tested under the same conditions, resulting in similar biomass conversions (Table S2†). All catalysts afford roughly equal lignin monomer yields, in the range of 47–50 wt% based on total lignin content (Fig. 4A). Noticeably, the monomer selectivity differs strongly, with the ratio of propanol-substituted monomers to propyl-substituted monomers decreasing in the order of Pd ≈ Ru > Pt ≫ Rh. These observations are also confirmed by GPC (Fig. S13†), ^{13}C-NMR (Fig. S8†), and HSQC NMR (Fig. S9†). Panel B of Fig. 4 summarises the composition of the aqueous fraction for the different noble metal catalysts. RCF with Ru/C yields the highest amounts of C5 polyols, equalling 48 mg $g_{biomass}^{-1}$ (Y = 25 C%) as analysed by GC-FID. Ru is known for its superior activity and selectivity in the hydrogenation of sugars,[61,77] and is frequently applied for hydrolytic hydrogenation of polysaccharides.[63,65–67] The C5 polyol yield for Pt/C is significantly lower (12 mg $g_{biomass}^{-1}$), while for Pd/C and Rh/C, almost no C5 nor C6 polyols were detected, as was also verified by HPLC analysis (Fig. S20†). The yield of carbohydrate oligomers follows a similar trend, suggesting that these are reduced oligomers. Overall, the studied carbon-supported catalysts perform equally well in terms of lignin monomer yield, but Ru/C outperforms the other catalysts when considering the yield of polyols in the aqueous fraction.

Similar experiments were conducted with Al_2O_3-supported noble metal catalysts (5 wt% metal loading). All the investi-
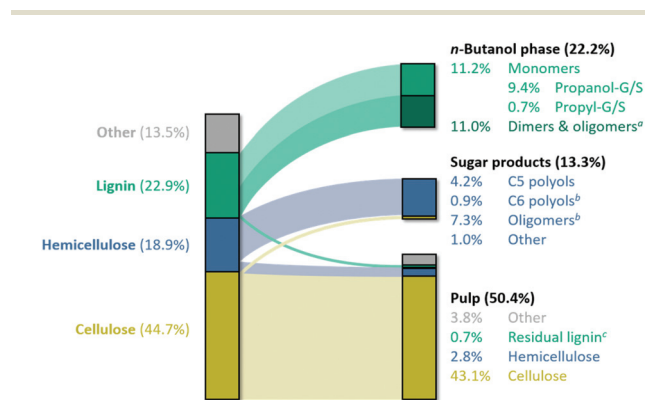

Fig. 3 Overview of the fractions obtained from RCF in *n*-butanol/water (right), in relation to the composition of the biomass (left). All numbers are expressed as wt% relative to the pre-extracted eucalyptus substrate. Reaction conditions: See Fig. 1. [a] Assuming that the *n*-butanol oil, apart from lignin monomers (Fig. 2A), solely consists of dimers and oligomers.

[b] It could not be resolved to what extent C6 polyols and oligomers originate from cellulose. The high retention of glucan in the pulp at least indicates that oligomers mainly originate from hemicellulose.
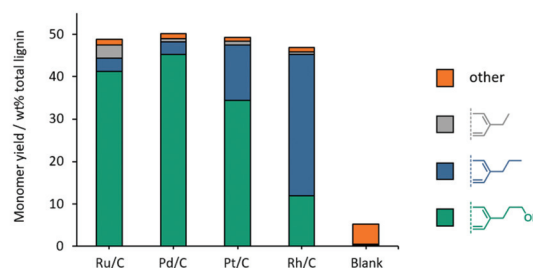
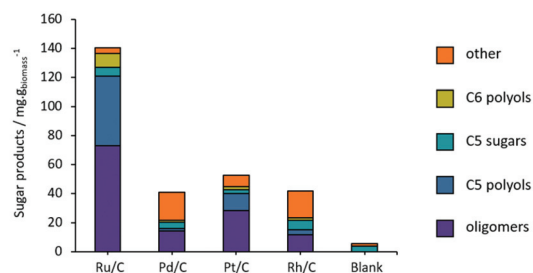[c] Estimated based on the *n*-butanol oil yield.

Fig. 4 (A) Lignin monomers (B) and carbohydrate products obtained from RCF in *n*-butanol/water with different catalysts. Reaction conditions: 20 mL *n*-butanol, 20 mL water, 2 g pre-extracted eucalyptus sawdust, 0.2 g catalyst, 30 bar H_2, 200 °C, 2 h.
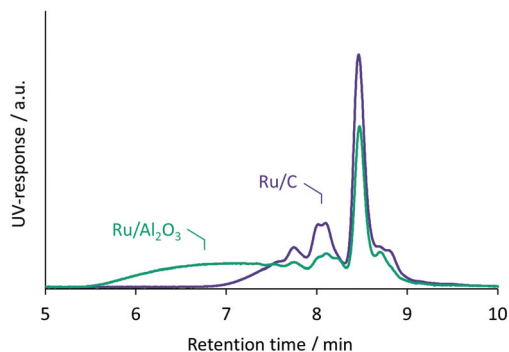
Fig. 5 GPC of lignin product oil (*n*-butanol phase) obtained with Ru/C and Ru/Al$_2$O$_3$. Reaction conditions: 20 mL *n*-butanol, 20 mL water, 2 g pre-extracted eucalyptus sawdust, 0.2 g catalyst, 30 bar H$_2$, 200 °C, 2 h. GPC chromatograms for other noble metal catalysts (on C and Al$_2$O$_3$) are provided in Fig. S14.†

Fig. 6 Influence of Ru/C loading and recycling on (A) obtained lignin monomers and (B) aqueous carbohydrate products. Reaction conditions: 40 mL solvent, 2 g pre-extracted eucalyptus sawdust, 30 bar H$_2$, 200 °C, 2 h. For experimental details on Ru/C recycling, the reader is referred to the ESI.†

gated alumina catalysts exhibit lower lignin monomer yields compared to their carbon-supported counterparts (Table S2†). GPC analysis demonstrates the presence of a high molecular weight fraction in the lignin oils from the Al$_2$O$_3$-based catalysts (Fig. 5 and S14†), indicating less efficient depolymerisation compared to the carbon-based catalysts. Moreover, Ru/Al$_2$O$_3$ affords a lower C5 polyol yield than Ru/C (28 *vs.* 48 mg g$_{biomass}$$^{-1}$). The reason for the better performance of the carbon-supported catalysts was not further investigated. Possible hypotheses are (i) the fact that γ-Al$_2$O$_3$ in aqueous environments can phase-transform into boehmite, thereby encapsulating metal particles,[12] or (ii) a less favourable interaction between Al$_2$O$_3$ and lignin, hemicellulose, and/or hydrogen, eventually resulting in lower product yields.[61]

A control run without catalyst and pressurised hydrogen (referred to as '*blank*') was executed. The lignin monomer yield only reached 5 wt% (Fig. 4A). GPC shows that the dark oil obtained upon evaporation of *n*-butanol mainly comprises oligomers (Fig. S15†), resulting from repolymerisation.[45] As expected, no significant quantities of C5 polyols, sugars, or oligomers were detected in the aqueous phase. The results of the blank run unambiguously justify the implementation of a redox catalyst, preferably Ru/C, which is needed to hydrogenate reactive intermediates into stable products (*i.e.* phenolics and polyols).

In addition to the catalyst type, experiments were performed to investigate the effect of decreasing the catalyst-to-biomass ratio, which is more desirable for industrial operation. Therefore, the process was operated with different amounts of Ru/C, in the range of 0.2–0.02 g (Fig. 6). Lowering the Ru/C loading from 0.2 g (reference conditions, Fig. 1) to 0.1 g has only a minor effect on both the lignin monomer yield and C5 polyol yield. Hence, the *n*-butanol/water RCF process works effectively with 5 wt% Ru/C relative to the biomass, which corresponds to 0.25 wt% metal. Further lowering the amount of Ru/C negatively impacts the conversion of lignocellulose. The lignin monomer yield decreases down to 39.1 wt% (0.05 g Ru/C) and 17.6 wt% (0.02 g Ru/C), indicating
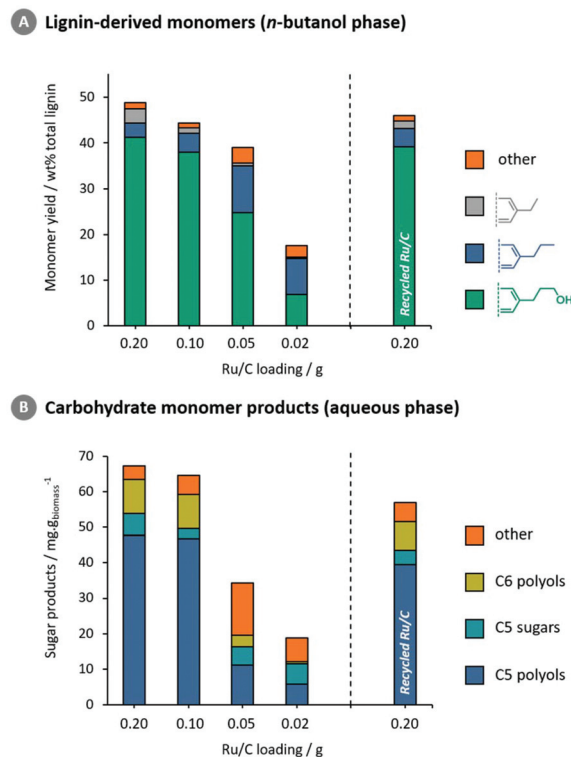
that lignin depolymerisation-stabilisation becomes less effective. In addition, also the selectivity towards propanol-substituted monomers decreases with decreasing catalyst-to-biomass ratio (Fig. 6A). Both effects are confirmed by GPC (Fig. S16†). Likewise, also the C5 polyol yield and selectivity drop when the loading of Ru/C equals 0.05 g or less.

Catalyst recuperation is an important but challenging aspect given the fact that RCF involves a solid substrate and a solid redox catalyst. Different catalyst recuperation strategies have been disclosed, which were recently reviewed by Barta and co-workers.[10,78] Briefly, these include the use of ferromagnetic catalysts,[42,79,80] catalyst pellets,[45] a catalyst basket,[45,81] or a flow-through reactor.[38,46,76] In this work, liquid–liquid extraction was applied to separate the catalyst from the pulp. Therefore, the residual solids were washed with *n*-butanol and water (ESI†). The carbon-supported catalyst is relatively apolar and primarily resides in the *n*-butanol phase. The pulp on the other hand is located at the bottom of the aqueous phase. In this way, a black powder could be isolated that corresponds to 98.1 wt% of the initial Ru/C, in addition to a pale pulp (96.4 wt%, Fig. S10†). Subsequently, the standard RCF experiment (Fig. 1) was conducted with the recovered Ru/C. The recycled catalyst provided a quasi-similar lignin monomer yield (46.0 wt%) compared to fresh Ru/C (48.8 wt%), with high selectivity towards propanol-substituted

monomers (Fig. 6A). The obtained C5 polyol yield is slightly lower (40 vs. 48 mg g^{-1} biomass), whereas the pulp yield is similar (48.8 vs. 50.4 wt%). To conclude, this recycle experiment confirms that the spent Ru/C can be reused and displays good catalytic activity. Further research concerning catalyst stability and deactivation is strongly encouraged. Flow-through reactors are particularly suited for this.[76]

Influence of hydrogen pressure & reaction network

In addition to the redox catalyst, also the hydrogen partial pressure determines the outcome of the n-butanol/water RCF process. To investigate its impact on the ongoing chemistry, the process was performed under different hydrogen pressures, between 0 and 50 bar H_2. Without external hydrogen (30 bar N_2), the Ru/C-catalysed RCF process selectively yields propenyl-substituted monomers (Fig. 7A). Despite the high monomer selectivity, the total monomer yield is rather low (17 wt%), indicating inefficient stabilisation of reactive intermediates. This is confirmed by GPC analysis, which shows a significant fraction of relatively large oligomers (Fig. S17†). Increasing the H_2 pressure from 0 to 10 bar strongly enhances the monomer yield. The monomers mainly comprise propyl- and propanol-substituted guaiacol/syringol, with the selectivity to propyl side-chains decreasing with increasing H_2 pressure.

A Lignin-derived monomers (n-butanol phase)

B Sugar-derived products (aqueous phase)

Fig. 7 (A) Lignin monomers and (B) aqueous carbohydrate products obtained from RCF in n-butanol/water with Ru/C and varying hydrogen pressure. Reaction conditions: 20 mL n-butanol, 20 mL water, 2 g pre-extracted eucalyptus sawdust, 0.2 g Ru/C, 200 °C, 2 h. Reaction in absence of H_2 was performed under 30 bar N_2.

The monomer yield is highest when a pressure in the range of 10–30 bar H_2 is applied. Under these conditions, propanol-substituted G/S are the predominant monomers. Above 30 bar H_2, the monomer yield slightly decreases. A recent study on NiFe/C-catalysed RCF also reported a decrease in monomer yield when exceeding a hydrogen pressure of 20 bar, the reason for which is unknown.[82]

The trends deduced from Fig. 7A lead to the construction of a reaction network for the reductive conversion of native lignin (Scheme 1). Recently, coniferyl and sinapyl alcohol were identified as key intermediates.[38,45,46,83] These unsaturated compounds can even be formed solvolytically (**R1**), in absence of a redox catalyst, and are unstable at elevated temperature.[45] Coniferyl and sinapyl alcohol serve as a pivotal point in Scheme 1. They can either undergo hydrogenation of the $C_\alpha{=}C_\beta$ bond to propanol-substituted G/S (**R2**); hydrogenolysis of the terminal hydroxy group to propenyl-substituted G/S (**R3**); or repolymerisation, yielding soluble lignin oligomers (**R4**).

In absence of pressurised hydrogen, the hydrogenolysis route (**R3**) prevails, as indicated by the high selectivity towards propenyl-substituted monomers (Fig. 7A). The solvent or solubilised carbohydrates likely serve as reducing agent.[47,53] However, the rather low monomer yield obtained in absence of pressurised hydrogen also indicates the occurrence of repolymerisation (**R4** and/or **R7**), which involves unsaturated side-chains.[38,45] Repolymerisation can be prevented by hydrogenating these unsaturated bonds,[38,45] thereby yielding stable phenolic products. Under relatively low hydrogen pressure (5 bar), hydrogenolysis of coniferyl/sinapyl alcohol (**R3**) and subsequent hydrogenation (**R6**) constitutes the major reaction pathway, resulting in propyl-substituted monomers (Fig. 7A). On the other hand, direct hydrogenation (**R2**) of coniferyl/sinapyl alcohol becomes more predominant with increasing hydrogen pressure, thus selectively yielding propanol-substituted monomers. This selectivity change can be explained by the fact that hydrogenolysis reactions are typically negative order in hydrogen pressure, in contrast to hydrogenation reactions.[84]
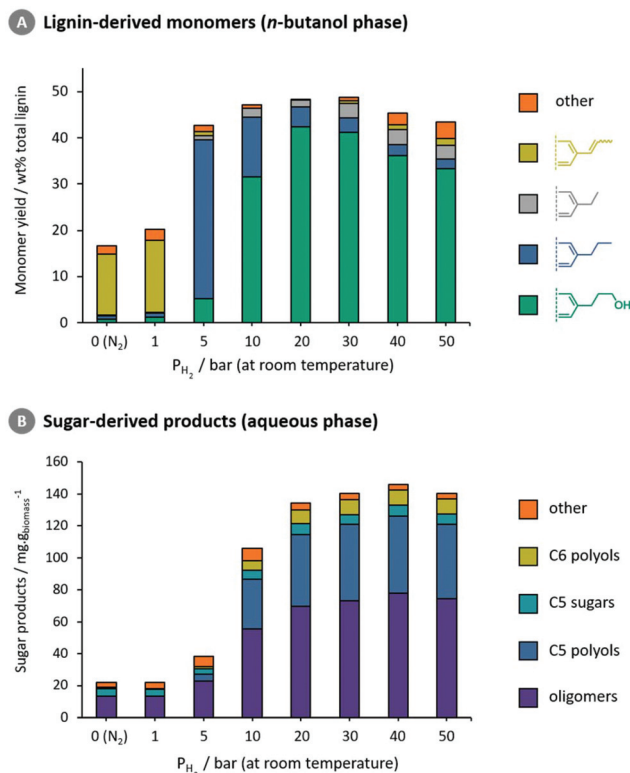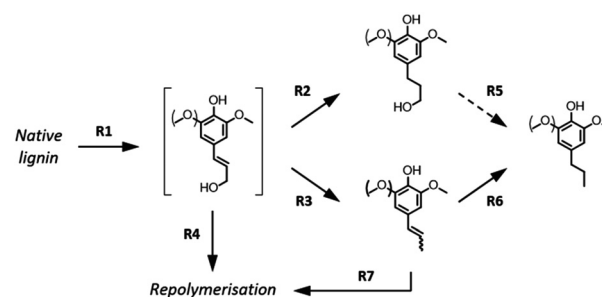
Scheme 1 Proposed reaction network of lignin depolymerisation to phenolic monomers. Under the studied reaction conditions, formation of propyl-substituted monomers occurs primarily through the lower pathway (**R3** + **R6**), which predominates under low hydrogen pressure. Direct hydrogenation (**R2**) yielding propanol-substituted compounds is favoured under high hydrogen pressure (Fig. 7A).

In addition, it was observed that increasing the contact time (by applying a higher catalyst loading) did not increase the selectivity towards propyl-substituted monomers, not even at low H_2 pressure (10 bar, Fig. S6†). This indicates that propanol side-chains are not readily converted to propyl side-chains under the studied reaction conditions (**R5**). We therefore conclude that formation of propyl-substituted monomers occurs primarily through pathway **R3** + **R6**, *i.e.* coniferyl/sinapyl alcohol hydrogenolysis, followed by hydrogenation of the $C_\alpha = C_\beta$ bond. This insight may guide future research to gain control over the proposed reaction network, for instance through catalyst and process design.

Finally, the effect of hydrogen pressure on the carbohydrate products in the aqueous phase is illustrated in Fig. 7B. In absence of pressurised hydrogen, the yield of targeted carbohydrate products is low, which is ascribed to degradation (as indicated by the yellowish colour of the aqueous phase). With increasing pressure, the yield of (stable) C5 polyols gradually increases and reaches a plateau at 20 bar. The yield of carbohydrate oligomers follows a similar trend, as analysed by HPLC (Fig. 7B). Stabilisation (*i.e.* hydrogenation) of solubilised hemicellulose thus requires a higher hydrogen pressure than stabilisation of lignin. At relatively low hydrogen pressure, lignin stabilisation proceeds effectively through the hydrogenolysis–hydrogenation pathway (**R3** + **R6** in Scheme 1), and close-to-theoretical monomer yields are already obtained under 5 bar H_2. Overall, 20–30 bar H_2 is the optimal pressure range to acquire high yields of both phenolics and C5 polyols.

Influence and stability of the solvent

To illustrate the requirement of both solvents, RCF of eucalyptus with Ru/C was performed in pure *n*-butanol and pure water. After reaction, a similar work-up procedure (ESI†) was performed so that each reaction resulted in an *n*-butanol phase and an aqueous phase (120 mL each).

When performing RCF in pure *n*-butanol, the biomass conversion and lignin oil yield measured 10.1 wt% and 5.6 wt% respectively, in contrast to 49.6 wt% and 22.2 wt% for the mixed solvent system. Hence, pure *n*-butanol is not effective for the intended RCF process, which is also reflected by the low lignin monomer yield (7.9 wt% on lignin basis, Fig. 8A) and insignificant amounts of carbohydrate products in the aqueous phase (Fig. 8B).

Performing the RCF process in pure water affords a higher lignin monomer yield (35.0 wt%) and oil yield (13.6 wt% of initial biomass) compared to processing in pure *n*-butanol. Notwithstanding, product yields are lower compared to the mixed solvent system. On the other hand, the yield of C5 polyols is *circa* threefold higher for the reaction in water compared to the mixed solvent system (Fig. 8B). This observation is ascribed to the higher polarity of pure water, which facilitates hemicellulose hydrolysis, as evidenced by the near absence of oligomers (HPLC, Fig. S21†). More strikingly is the fact that lignin depolymerisation in pure water is less selective, with a significant fraction of the monomers comprising propylcyclohexanol and ethylcyclohexanol (Fig. 8A). We reason
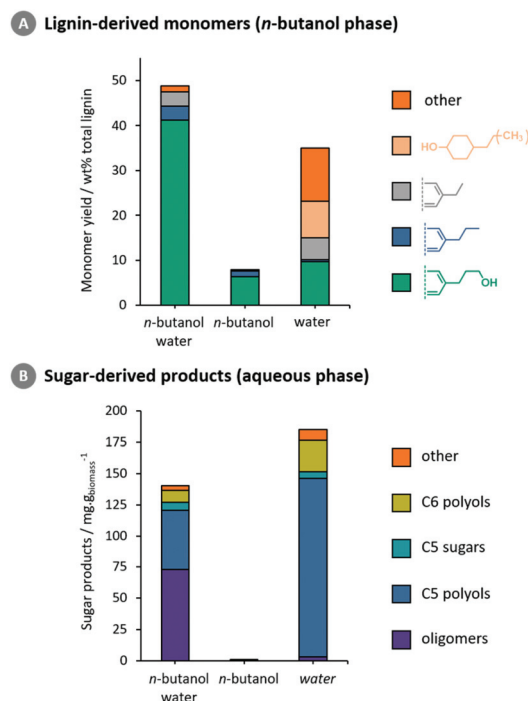

Fig. 8 Influence of RCF solvent composition on (A) obtained lignin monomers and (B) aqueous carbohydrate products. Reaction conditions: 40 mL solvent, 2 g pre-extracted eucalyptus sawdust, 0.2 Ru/C, 30 bar H_2, 200 °C, 2 h. After reaction, an extraction procedure (ESI†) was executed so that each reaction resulted in an *n*-butanol phase and an aqueous phase (120 mL each).

that the sorption behaviour of phenolics on the catalyst surface is either directly or indirectly affected by the presence of *n*-butanol. In support, Lercher and co-workers recently reported that hydrogenation of phenol proceeds faster in water than in methanol, which was ascribed to (i) better solvation of phenol by the alcohol solvent, and (ii) adsorption of the alcohol on the hydrogenation catalyst.[85] The utilisation of an alcohol solvent thus protects the phenolic monomers from undergoing ring hydrogenation and subsequent demethoxylation, at least in presence of Ru/C.[86] Overall, a mixture of *n*-butanol/water affords higher lignin oil and monomer yields compared to either pure *n*-butanol or pure water, which is in line with RCF studies on methanol/water[52,87] and ethanol/water.[52]

An important aspect for industrial operation is the stability of *n*-butanol during catalytic processing.[88] To uncover the main solvent degradation pathways, the headspace was analysed after performing the standard *n*-butanol/water RCF process (Fig. 1). The major gaseous products are methane and propane, whereas butane was only detected in minor quantities (Table 1). In extent, no significant concentrations of dibutyl ether (in liquid phase) were detected. Assuming that all the products originate from the solvent, 1.34 C% of *n*-butanol is lost under the standard reaction conditions. The main degradation products, propane and methane, likely originate from the cleavage of the C_α–C_β bond in *n*-butanol, as

Table 1 Analysis of the headspace after *n*-butanol/water RCF, indicating the main solvent degradation products. Reaction conditions: 20 mL *n*-butanol, 20 mL water, 2 g pre-extracted eucalyptus sawdust, 0.2 g Ru/C, 30 bar H_2, 200 °C, 2 h

Compound	Vol%	C% *n*-butanol[a]
N_2	4.40	—
H_2	84.20	—
Methane	5.08	0.28
Ethane	0.06	0.01
Propane	6.22	1.04
Butane	0.04	0.01
Total		**1.34**

[a] Assuming that all carbonaceous gasses originate from *n*-butanol.

suggested by earlier work using Ru/C.[89] The occurrence of methane and propane in similar volumetric amounts strengthens this hypothesis. Note that an analogous reaction explains the formation of ethyl-substituted compounds from propanol-substituted monomers.[34] A possible strategy to mitigate this side-reaction would be to lower the catalyst loading (Fig. 6) or to alter the catalyst properties.

Improved hemicellulose hydrolysis: implementing acidity (HCl)

In the *proof-of-concept* experiment (Fig. 1), 85 wt% of the hemicellulose was removed, though the solubilised oligomers were only partly converted into C5 polyols (*vide supra*, Fig. 2).

Carbohydrate hydrolysis is thus the rate determining step under these standard reaction conditions. To improve the hydrolysis of carbohydrate oligomers, the implementation of HCl was investigated.

In a first set of experiments, the standard *n*-butanol/water RCF process (200 °C) was performed with different amounts of HCl, in the range of 25–100 µmol (in 40 mL solvent mixture). The addition of HCl leads to an increased solubilisation of hemicellulose, from 85 wt% up to 94 wt%, while the cellulose fraction remains effectively retained in the pulp (~90 wt%). The yield of C5 polyols gradually increases with increasing acidity (Fig. 9B), from 48 g $g_{biomass}^{-1}$ (Y = 25 C%) under neutral conditions to 113 mg $g_{biomass}^{-1}$ (Y = 60 C%) when adding 100 µmol HCl. The total lignin monomer yield remains similar (in the range of 46.1–49.0 wt%). The selectivity towards propanol-substituted phenolics slightly decreases, from 85 wt% down to 73 wt%.

Subsequently, we investigated if it is possible to perform the RCF process at lower temperature by adding higher amounts of HCl, since it is known that acidic additives promote both hemicellulose hydrolysis and delignification during RCF.[39,40,54,90] Similar experiments were therefore conducted at 180 °C (0–200 µmol HCl) and 160 °C (0–400 µmol HCl). Results of this investigation are summarised in Fig. 9. In neutral conditions, the *n*-butanol oil yield and lignin monomer yield decrease with decreasing temperature, pointing out incomplete delignification below 200 °C.
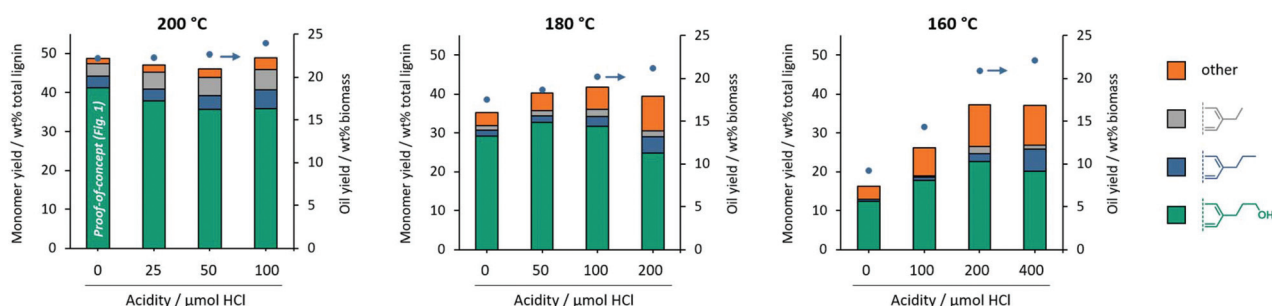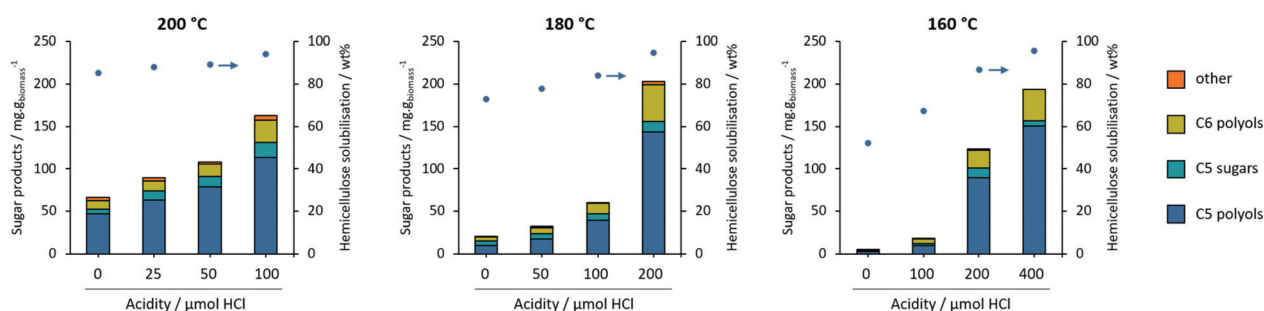

Fig. 9 Summary of the implementation of HCl in *n*-butanol/water RCF. (A) Yield of lignin monomers in *n*-butanol phase and (B) carbohydrate monomer products in aqueous phase. For each reaction temperature (160, 180 and 200 °C), a different acidity range was investigated. Reaction conditions: 20 mL *n*-butanol, 20 mL water, 2 g pre-extracted eucalyptus sawdust, 0.2 g Ru/C, 30 bar H_2, 2 h. The *n*-butanol oil yield or degree of hemicellulose solubilisation is displayed on the secondary *y*-axis.

The *n*-butanol oil yield was increased by adding HCl, thus showing that extensive biomass delignification can even be achieved at 160 °C (Fig. 9A). At temperatures below 200 °C, also the lignin monomer yield increases with increasing acidity, but remains well below 48.8 wt%, which is the yield obtained under standard conditions (200 °C, neutral). Acid-catalysed condensation may become more significant at high acid loadings, thereby reducing the total monomer yield. Moreover, high acid loadings ($\geq$200 µmol HCl) negatively affect the selectivity towards propanol-G/S due to acid-catalysed side reactions. For instance, the fraction of propyl-substituted compounds increases, which is ascribed to acid-catalysed dehydration of the γ-OH group followed by hydrogenation. Another side reaction is the acid-catalysed etherification of the γ-OH group with *n*-butanol, leading to the formation of etherified monomers, the highest yield (3.7 wt%) of which was obtained at 160 °C with 400 µmol HCl. Overall, lignin disassembly is less effective and less selective under *low temperature – high acidity* conditions than under *high temperature – low acidity* conditions. This observation was also verified by GPC analysis. The chromatogram of the oil obtained at 160 °C (400 µmol HCl) displays relatively more oligomers and a smaller propanol-G/S signal compared to the oil obtained at 200 °C (100 µmol HCl).

Panel B of Fig. 9 depicts the yield of carbohydrate monomer products in the aqueous phase, in function of temperature and acidity. At all three temperatures, the yield of targeted C5 polyols increases with increasing acidity. The highest yield of C5 polyols equals 150 mg $g_{biomass}^{-1}$ (80 C%), and was obtained at 160 °C with 400 µmol HCl. This yield is similar to the C5 polyol yield obtained in pure water at 200 °C (143 mg $g_{biomass}^{-1}$, Fig. 8B). Note that each temperature-acidity combination results in a unique process severity and therefore a different hemicellulose conversion. A comparison is therefore not straightforward. To overcome this issue, the C5 polyol yield was plotted in function of C5 solubilisation (Fig. 10B), which is a measure for hemicellulose conversion. Fig. 10B shows an exponential increase of the C5 polyol yield in function of C5 solubilisation. The deviation from the theoretical 1 : 1 conversion–yield relationship indicates that oligomers predominate under low severity conditions. Oligomer hydrolysis thus occurs more slowly and requires more severe conditions than hemicellulose solubilisation. Furthermore, the data points in Fig. 10B form one exponential curve, independent of temperature. This suggests that hydrolytic hydrogenation of hemicellulose during RCF is rather a function of process severity in general, in contrast to lignin conversion, which is favoured at high temperature – low acidity (*vide supra*, Fig. 10A), at least under the studied conditions. Overall, these experiments show that small amounts of HCl can assist the envisioned catalytic biorefinery process, though, balancing the different parameters that determine process severity is key (*i.e.* temperature, acidity, reaction time).[91]
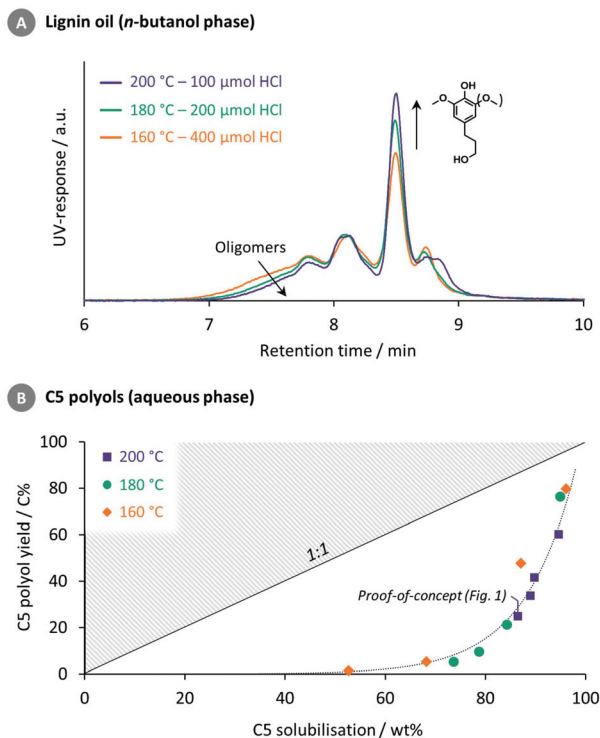
Conclusions

In this contribution, a catalytic biorefinery approach is proposed, targeting the fractionation of lignocellulosic biomass into (i) lignin-derived (mono)phenolics, (ii) hemicellulose-derived polyols, and (iii) a cellulosic pulp. Biomass processing is performed in an equivolumetric mixture of *n*-butanol and water at 200 °C, in presence of a reductive catalytic system. The co-solvent mixture enables extraction and depolymerisation of both lignin and hemicellulose, whereas the catalyst's role is to convert reactive species (lignin fragments and sugars) into stable target products (phenolics and polyols, respectively). Cooling of the reaction liquor induces phase separation, thereby providing an integrated separation of phenolics (*n*-butanol phase) and polyols (aqueous phase). The cellulose fraction is easily retrieved as a pulp upon filtration. A *proof-of-concept* using a 2 L batch reactor demonstrates the scalability potential of the process.

In a broader context, this work shows that simultaneous valorisation of both lignin and hemicellulose in a catalytic biorefinery is feasible, but one should take into account that appropriate reaction conditions may be different for each biopolymer. For instance, it was shown that the catalyst, hydrogen pressure, solvent composition, temperature and acidity have different consequences for lignin as for hemicellulose conversion. Finding a window that enables (close-to-)optimal valorisation of all targeted constituents is a key challenge.

Fig. 10 (A) GPC of lignin product oil (*n*-butanol phase) obtained with different temperature-[HCl] combinations. Additional chromatograms are shown in Fig. S18 and 19.† (B) C5 polyol yield in function of C5 solubilisation (*i.e.* xylan and arabinan). For a representation with *temperature-acidity* labels: see Fig. S22.†

Experimental section

For a list of all used chemicals and materials as well as a more complete description of the experimental procedures, the reader is kindly referred to the ESI.†

Dry eucalyptus wood chips were milled and sieved to obtain a sawdust fraction with a size of 250–500 μm. Subsequently, a two-step extraction procedure was followed using a Soxtec 2055 Avanti apparatus to remove any extractives (*circa* 1 wt% on wood basis). This sawdust, hereinafter referred to as 'pre-extracted sawdust', was used for catalytic experiments. The composition is summarised in Table S1.† Compositional analysis of the eucalyptus sawdust was performed by NREL according to NREL *Laboratory Analytical Procedures*.[92–95]

RCF experiments were performed in a 100 ml stainless steel batch reactor (*Parr Instruments & Co.*). In a typical reaction, 2 g pre-extracted sawdust was loaded into the reactor together with the catalyst powder (0.2 g Ru/C or other) and a solvent mixture (40 mL) comprising *n*-butanol/water in equal volumetric amounts. The reactor was sealed, flushed threefold with N_2, and pressurised with H_2 (typically 30 bar at room temperature). The reaction mixture was stirred (750 rpm) and heated to 200 °C ($\sim$15 °C min^{-1}). When the reaction temperature was reached, the temperature was kept constant for 2 h after which the reactor was cooled and depressurised at room temperature. Afterwards, the reactor contents were quantitatively collected by washing the reactor with water and *n*-butanol.

The obtained product mixture was filtered using a 30 mL Por 4. fritted glass filter to separate the solid residue (pulp and catalyst) from the liquid products. The solid pulp was washed with additional water and *n*-butanol so that the resulting filtrate was composed of 120 mL water and 53 mL *n*-butanol. The two phases of the filtrate were separated from each other using a 250 mL separatory funnel, as depicted in Fig. 1. Subsequently, the aqueous phase was washed two times with 33 mL *n*-butanol to fully extract the depolymerised lignin (see Fig. S1 in the ESI†). In this way, the total *n*-butanol fraction measured $\sim$120 mL, equal to the volume of the aqueous fraction.

The *n*-butanol was evaporated using a rotavap and yielded a viscous orange-brown lignin oil. The lignin oil was dried overnight at 80 °C, after which the mass of the dry oil could be determined. For quantitative determination of the monomers, 2-isopropylphenol was added as an internal standard and the oil was resolubilised in ethanol, followed by GC-FID analysis. GC-MS analysis was performed to verify the identification of the monomers. In addition, GPC, ^{13}C NMR, and HSQC NMR were performed to characterise the complete lignin oil.

The aqueous phase was analysed by GC-FID and HPLC-RI. *myo*-Inositol was added as an internal standard for quantification. A derivatisation step (*viz.* trimethylsilylation) was applied preceding GC-FID analysis to increase the volatility of the carbohydrate-derived products (*e.g.* sugars, polyols).

The carbohydrate content of the pulp was determined using a standard total sugar procedure, adapted with hydrolysis conditions for cellulose-rich materials. The essential steps of this procedure are (i) a two-step H_2SO_4-catalysed hydrolysis, (ii) reduction of the released sugars with $NaBH_4$, (iii) acetylation of the polyols with acetic anhydride, and (iv) extraction of the acetylated products with *in situ* formed ethyl acetate, followed by (v) GC-FID analysis. Each sample was analysed in triplicate.

Conflicts of interest

There are no conflicts to declare.

Acknowledgements

Notes and references

1 A. J. Ragauskas, C. K. Williams, B. H. Davison, G. Britovsek, J. Cairney, C. A. Eckert, W. J. Frederick, J. P. Hallett, D. J. Leak and C. L. Liotta, *Science*, 2006, **311**, 484–489.

2 R. D. Perlack and B. J. Stokes, *US billion-ton update: biomass supply for a bioenergy and bioproducts industry*, Report ORNL/TM-2011/224, Oak Ridge National Laboratory, Oak Ridge, TN, 2011.

3 W. Schutyser, T. Renders, S. Van den Bosch, S. F. Koelewijn, G. T. Beckham and B. F. Sels, *Chem. Soc. Rev.*, 2018, **47**, 852–908.

4 I. Delidovich, P. J. C. Hausoul, L. Deng, R. Pfützenreuter, M. Rose and R. Palkovits, *Chem. Rev.*, 2016, **116**, 1540–1599.

5 D. Esposito and M. Antonietti, *Chem. Soc. Rev.*, 2015, **44**, 5821–5835.

6 M. Pelckmans, T. Renders, S. Van de Vyver and B. F. Sels, *Green Chem.*, 2017, **19**, 5303–5331.

7 F. H. Isikgor and C. R. Becer, *Polym. Chem.*, 2015, **6**, 4497–4559.

8 C. Xu, R. A. D. Arancon, J. Labidi and R. Luque, *Chem. Soc. Rev.*, 2014, **43**, 7485–7500.

9 C. Li, X. Zhao, A. Wang, G. W. Huber and T. Zhang, *Chem. Rev.*, 2015, **115**, 11559–11624.

10 Z. Sun, B. Fridrich, A. de Santi, S. Elangovan and K. Barta, *Chem. Rev.*, 2018, **118**, 614–678.

11 P. Azadi, O. R. Inderwildi, R. Farnood and D. A. King, *Renewable Sustainable Energy Rev.*, 2013, **21**, 506–523.

12 R. Rinaldi, R. Jastrzebski, M. T. Clough, J. Ralph, M. Kennema, P. C. A. Bruijnincx and B. M. Weckhuysen, *Angew. Chem., Int. Ed.*, 2016, **55**, 8164–8215.

13 A. J. Ragauskas, G. T. Beckham, M. J. Biddy, R. Chandra, F. Chen, M. F. Davis, B. H. Davison, R. A. Dixon, P. Gilna, M. Keller, P. Langan, A. K. Naskar, J. N. Saddler, T. J. Tschaplinski, G. A. Tuskan and C. E. Wyman, *Science*, 2014, **344**, 1246843.

14 S. Gillet, M. Aguedo, L. Petitjean, A. R. C. Morais, A. M. da Costa Lopes, R. M. Lukasik and P. T. Anastas, *Green Chem.*, 2017, **19**, 4200–4233.

15 S.-F. Koelewijn, S. Van den Bosch, T. Renders, W. Schutyser, B. Lagrain, M. Smet, J. Thomas, W. Dehaen, P. Van Puyvelde, H. Witters and B. F. Sels, *Green Chem.*, 2017, **19**, 2561–2570.

16 S.-F. Koelewijn, C. Cooreman, T. Renders, C. A. Saiz, S. Van den Bosch, W. Schutyser, W. De Leger, M. Smet, P. Van Puyvelde, H. Witters, B. Van der Bruggen and B. F. Sels, *Green Chem.*, 2018, **20**, 1050–1058.

17 S. Constant, H. L. J. Wienk, A. E. Frissen, P. D. Peinder, R. Boelens, D. S. van Es, R. J. H. Grisel, B. M. Weckhuysen, W. J. J. Huijgen, R. J. A. Gosselink and P. C. A. Bruijnincx, *Green Chem.*, 2016, **18**, 2651–2665.

18 T. Renders, S. Van den Bosch, S. F. Koelewijn, W. Schutyser and B. F. Sels, *Energy Environ. Sci.*, 2017, **10**, 1551–1557.

19 L. da Costa Sousa, M. Foston, V. Bokade, A. Azarpira, F. Lu, A. J. Ragauskas, J. Ralph, B. Dale and V. Balan, *Green Chem.*, 2016, **18**, 4205–4215.

20 L. da Costa Sousa, M. Jin, S. P. S. Chundawat, V. Bokade, X. Tang, A. Azarpira, F. Lu, U. Avci, J. Humpula, N. Uppugundla, C. Gunawan, S. Pattathil, A. M. Cheh, N. Kothari, R. Kumar, J. Ralph, M. G. Hahn, C. E. Wyman, S. Singh, B. A. Simmons, B. E. Dale and V. Balan, *Energy Environ. Sci.*, 2016, **9**, 1215–1223.

21 A. Mittal, R. Katahira, B. S. Donohoe, S. Pattathil, S. Kandemkavil, M. L. Reed, M. J. Biddy and G. T. Beckham, *ACS Sustainable Chem. Eng.*, 2017, **5**, 2544–2561.

22 J. S. Luterbacher, A. Azarpira, A. H. Motagamwala, F. C. Lu, J. Ralph and J. A. Dumesic, *Energy Environ. Sci.*, 2015, **8**, 2657–2663.

23 J. S. Luterbacher, J. M. Rand, D. M. Alonso, J. Han, J. T. Youngquist, C. T. Maravelias, B. F. Pfleger and J. A. Dumesic, *Science*, 2014, **343**, 277–280.

24 A. Brandt, J. Grasvik, J. P. Hallett and T. Welton, *Green Chem.*, 2013, **15**, 550–583.

25 L. Weigand, S. Mostame, A. Brandt, T. Welton and J. Hallett, *Faraday Discuss.*, 2017, **202**, 331–349.

26 J. Shi, S. Pattathil, R. Parthasarathi, N. A. Anderson, J. I. Kim, S. Venketachalam, M. G. Hahn, C. Chapple, B. A. Simmons and S. Singh, *Green Chem.*, 2016, **18**, 4884–4895.

27 C. S. Lancefield, I. Panovic, P. J. Deuss, K. Barta and N. J. Westwood, *Green Chem.*, 2017, **19**, 202–214.

28 P. J. Deuss, C. S. Lancefield, A. Narani, J. G. de Vries, N. J. Westwood and K. Barta, *Green Chem.*, 2017, **19**, 2774–2782.

29 S. Bauer, H. Sorek, V. D. Mitchell, A. B. Ibáñez and D. E. Wemmer, *J. Agric. Food Chem.*, 2012, **60**, 8203–8212.

30 D. V. Evtuguin, C. P. Neto, A. M. S. Silva, P. M. Domingues, F. M. L. Amado, D. Robert and O. Faix, *J. Agric. Food Chem.*, 2001, **49**, 4252–4261.

31 A. T. Smit and W. J. J. Huijgen, *Green Chem.*, 2017, **19**, 5505–5514.

32 D. Weidener, H. Klose, W. Leitner, U. Schurr, B. Usadel, P. Domínguez de María and P. M. Grande, *ChemSusChem*, 2018, **11**, 2051–2056.

33 L. Shuai, M. T. Amiri, Y. M. Questell-Santiago, F. Héroguel, Y. Li, H. Kim, R. Meilan, C. Chapple, J. Ralph and J. S. Luterbacher, *Science*, 2016, **354**, 329–333.

34 W. Lan, M. Talebi Amiri, C. M. Hunston and J. Luterbacher, *Angew. Chem., Int. Ed.*, 2018, **57**, 1356–1360.

35 K. H. Kim, B. A. Simmons and S. Singh, *Green Chem.*, 2017, **19**, 215–224.

36 F. P. Bouxin, A. McVeigh, F. Tran, N. J. Westwood, M. C. Jarvis and S. D. Jackson, *Green Chem.*, 2015, **17**, 1235–1242.

37 S. Van den Bosch, W. Schutyser, R. Vanholme, T. Driessen, S. F. Koelewijn, T. Renders, B. De Meester, W. J. J. Huijgen, W. Dehaen, C. M. Courtin, B. Lagrain, W. Boerjan and B. F. Sels, *Energy Environ. Sci.*, 2015, **8**, 1748–1763.

38 E. M. Anderson, M. L. Stone, R. Katahira, M. Reed, G. T. Beckham and Y. Román-Leshkov, *Joule*, 2017, **1**, 613–622.

39 T. Renders, W. Schutyser, S. Van den Bosch, S.-F. Koelewijn, T. Vangeel, C. M. Courtin and B. F. Sels, *ACS Catal.*, 2016, **6**, 2055–2066.

40 E. M. Anderson, R. Katahira, M. Reed, M. G. Resch, E. M. Karp, G. T. Beckham and Y. Roman-Leshkov, *ACS Sustainable Chem. Eng.*, 2016, **4**, 6940–6950.

41 X. Huang, O. M. Morales Gonzalez, J. Zhu, T. I. Koranyi, M. D. Boot and E. J. M. Hensen, *Green Chem.*, 2017, **19**, 175–187.

42 P. Ferrini, C. A. Rezende and R. Rinaldi, *ChemSusChem*, 2016, **9**, 3171–3180.

43 P. Ferrini and R. Rinaldi, *Angew. Chem., Int. Ed.*, 2014, **53**, 8634–8639.

44 M. V. Galkin and J. S. M. Samec, *ChemSusChem*, 2016, **9**, 1544–1558.

45 S. Van den Bosch, T. Renders, S. Kennis, S.-F. Koelewijn, G. Van den Bossche, T. Vangeel, A. Deneyer, D. Depuydt, C. M. Courtin, J. Thevelein, W. Schutyser and B. F. Sels, *Green Chem.*, 2017, **19**, 3313–3326.

46 I. Kumaniaev, E. Subbotina, J. Savmarker, M. Larhed, M. V. Galkin and J. Samec, *Green Chem.*, 2017, **19**, 5767–5771.

47 Q. Song, F. Wang, J. Cai, Y. Wang, J. Zhang, W. Yu and J. Xu, *Energy Environ. Sci.*, 2013, **6**, 994–1007.

48 S. Van den Bosch, W. Schutyser, S. F. Koelewijn, T. Renders, C. M. Courtin and B. F. Sels, *Chem. Commun.*, 2015, **51**, 13158–13161.

49 T. Parsell, S. Yohe, J. Degenstein, T. Jarrell, I. Klein, E. Gencer, B. Hewetson, M. Hurt, J. I. Kim, H. Choudhari, B. Saha, R. Meilan, N. Mosier, F. Ribeiro, W. N. Delgass, C. Chapple, H. I. Kenttamaa, R. Agrawal and M. M. Abu-Omar, *Green Chem.*, 2015, **17**, 1492–1499.

50 Y. Huang, Y. Duan, S. Qiu, M. Wang, C. Ju, H. Cao, Y. Fang and T. Tan, *Sustainable Energy Fuels*, 2018, **2**, 637–647.

51 N. Yan, C. Zhao, P. J. Dyson, C. Wang, L. T. Liu and Y. Kou, *ChemSusChem*, 2008, **1**, 626–629.

52 T. Renders, S. Van den Bosch, T. Vangeel, T. Ennaert, S.-F. Koelewijn, G. Van den Bossche, C. M. Courtin, W. Schutyser and B. F. Sels, *ACS Sustainable Chem. Eng.*, 2016, **4**, 6894–6904.

53 M. V. Galkin, A. T. Smit, E. Subbotina, K. A. Artemenko, J. Bergquist, W. J. J. Huijgen and J. S. M. Samec, *ChemSusChem*, 2016, **9**, 3280–3287.

54 X. Huang, X. Ouyang, B. Hendriks, O. Morales, J. Zhu, T. I. Koranyi, M. Boot and E. J. M. Hensen, *Faraday Discuss.*, 2017, **202**, 141–156.

55 W. Schutyser, S. Van den Bosch, T. Renders, T. De Boe, S. F. Koelewijn, A. Dewaele, T. Ennaert, O. Verkinderen, B. Goderis, C. M. Courtin and B. F. Sels, *Green Chem.*, 2015, **17**, 5035–5045.

56 T. Werpy, G. Petersen, A. Aden, J. Bozell, J. Holladay, J. White, A. Manheim, D. Eliot, L. Lasure and S. Jones, *Top value added chemicals from biomass. Volume 1-Results of screening for potential candidates from sugars and synthesis gas*, Report ADA436528, Department of Energy, Washington DC, 2004.

57 A. M. Ruppert, K. Weinberg and R. Palkovits, *Angew. Chem., Int. Ed.*, 2012, **51**, 2564–2601.

58 A. K. Beine, A. J. D. Kruger, J. Artz, C. Weidenthaler, C. Glotzbach, P. J. C. Hausoul and R. Palkovits, *Green Chem.*, 2018, **20**, 1316–1322.

59 A. Fukuoka and P. L. Dhepe, *Angew. Chem., Int. Ed.*, 2006, **45**, 5161–5163.

60 J. Geboers, S. Van de Vyver, K. Carpentier, P. Jacobs and B. Sels, *Green Chem.*, 2011, **13**, 2167–2174.

61 W. Deng, X. Tan, W. Fang, Q. Zhang and Y. Wang, *Catal. Lett.*, 2009, **133**, 167.

62 H. Kobayashi, Y. Ito, T. Komanoya, Y. Hosaka, P. L. Dhepe, K. Kasai, K. Hara and A. Fukuoka, *Green Chem.*, 2011, **13**, 326–333.

63 R. Palkovits, K. Tajvidi, A. M. Ruppert and J. Procelewska, *Chem. Commun.*, 2011, **47**, 576–578.

64 S. Liu, Y. Okuyama, M. Tamura, Y. Nakagawa, A. Imai and K. Tomishige, *Green Chem.*, 2016, **18**, 165–175.

65 T. Ennaert, S. Feys, D. Hendrikx, P. A. Jacobs and B. F. Sels, *Green Chem.*, 2016, **18**, 5295–5304.

66 K. Dietrich, C. Hernandez-Mejia, P. Verschuren, G. Rothenberg and N. R. Shiju, *Org. Process Res. Dev.*, 2017, **21**, 165–170.

67 D. Y. Murzin, B. Kusema, E. V. Murzina, A. Aho, A. Tokarev, A. S. Boymirzaev, J. Wärnå, P. Y. Dapsens, C. Mondelli, J. Pérez-Ramírez and T. Salmi, *J. Catal.*, 2015, **330**, 93–105.

68 D. Y. Murzin, E. V. Murzina, A. Tokarev, N. D. Shcherban, J. Wärnå and T. Salmi, *Catal. Today*, 2015, **257**, 169–176.

69 L. Faba, B. T. Kusema, E. V. Murzina, A. Tokarev, N. Kumar, A. Smeds, E. Díaz, S. Ordóñez, P. Mäki-Arvela, S. Willför, T. Salmi and D. Y. Murzin, *Microporous Mesoporous Mater.*, 2014, **189**, 189–199.

70 T. Ennaert, B. Op de Beeck, J. Vanneste, A. T. Smit, W. J. J. Huijgen, A. Vanhulsel, P. A. Jacobs and B. F. Sels, *Green Chem.*, 2016, **18**, 2095–2105.

71 H. Kobayashi, Y. Yamakoshi, Y. Hosaka, M. Yabushita and A. Fukuoka, *Catal. Today*, 2014, **226**, 204–209.

72 A. Yamaguchi, O. Sato, N. Mimura, Y. Hirosaki, H. Kobayashi, A. Fukuoka and M. Shirai, *Catal. Commun.*, 2014, **54**, 22–26.

73 A. Yamaguchi, O. Sato, N. Mimura and M. Shirai, *Catal. Today*, 2016, **265**, 199–202.

74 Q. Liu, T. Zhang, Y. Liao, C. Cai, J. Tan, T. Wang, S. Qiu, M. He and L. Ma, *ACS Sustainable Chem. Eng.*, 2017, **5**, 5940–5950.

75 A. F. Barton, *Alcohols with Water: Solubility Data Series*, Elsevier, 2013.

76 E. M. Anderson, M. L. Stone, M. J. Hülsey, G. T. Beckham and Y. Román-Leshkov, *ACS Sustainable Chem. Eng.*, 2018, **6**, 7951–7959.

77 J. A. Geboers, S. Van de Vyver, R. Ooms, B. Op de Beeck, P. A. Jacobs and B. F. Sels, *Catal. Sci. Technol.*, 2011, **1**, 714–726.

78 Z. Sun and K. Barta, *Chem. Commun.*, 2018, **54**, 7725–7745.

79 Z. Cao, M. Dierks, M. T. Clough, I. B. Daltro de Castro and R. Rinaldi, *Joule*, 2018, **2**, 1118–1133.

80 C. Chesi, I. B. D. de Castro, M. T. Clough, P. Ferrini and R. Rinaldi, *ChemCatChem*, 2016, **8**, 2079–2088.

81 M. V. Galkin and J. S. M. Samec, *ChemSusChem*, 2014, **7**, 2154–2158.

82 Y. Zhai, C. Li, G. Xu, Y. Ma, X. Liu and Y. Zhang, *Green Chem.*, 2017, **19**, 1895–1903.

83 X. Besse, Y. Schuurman and N. Guilhaume, *Appl. Catal., B*, 2017, **209**, 265–272.

84 H. Bernas, A. J. Plomp, J. H. Bitter and D. Y. Murzin, *Catal. Lett.*, 2008, **125**, 8.

85 J. He, C. Zhao and J. A. Lercher, *J. Catal.*, 2014, **309**, 362–375.

86 In case of Pd/C, the lignin monomer selectivity does not depend on the solvent. RCF with Pd/C and pressurised hydrogen selectively yields propanol-substituted monomers, also when pure water is used as solvent. See ref. 51, 52 and 55.

87 J. Chen, F. Lu, X. Si, X. Nie, J. Chen, R. Lu and J. Xu, *ChemSusChem*, 2016, **9**, 3353–3360.

88 J.-P. Lange, *ChemSusChem*, 2018, **11**, 997–1014.

89 B. Op de Beeck, M. Dusselier, J. Geboers, J. Holsbeek, E. Morre, S. Oswald, L. Giebeler and B. F. Sels, *Energy Environ. Sci.*, 2015, **8**, 230–240.

90 X. Huang, J. Zhu, T. I. Korányi, M. D. Boot and E. J. M. Hensen, *ChemSusChem*, 2016, **9**, 3262–3267.

91 M. Galbe and G. Zacchi, in *Biofuels*, ed. L. Olsson, Springer Berlin Heidelberg, Berlin, Heidelberg, 2007, pp. 41–65.

92 *National Renewable Energy Laboratory, Biomass Compositional Analysis Laboratory Procedures*, https://www.nrel.gov/bioenergy/biomass-compositional-analysis.html, (accessed accessed March 2018).

93 A. Sluiter, B. Hames, R. Ruiz, C. Scarlata, J. Sluiter, D. Templeton and D. Crocker, *Determination of Structural Carbohydrates and Lignin in Biomass*, Report NREL/TP-510-42618, National Renewable Energy Laboratory, Golden, CO, 2008 (revised 2012).

94 A. Sluiter, R. Ruiz, C. Scarlata, J. Sluiter and D. Templeton, *Determination of Extractives in Biomass*, Report NREL/TP-510-42619, National Renewable Energy Laboratory, Golden, CO, 2005.

95 J. Sluiter and A. Sluiter, *Summative Mass Closure*, Report NREL/TP-510-48087, National Renewable Energy Laboratory, Golden, CO, 2010 (revised 2011).